

# $Z'$ identification at the HE-LHC

Clement Helsens<sup>1</sup>, David Jamin<sup>2</sup>, Michelangelo L. Mangano<sup>3</sup>, Thomas G. Rizzo<sup>4</sup>, and Michele Selvaggi<sup>1</sup>

<sup>1</sup>CERN EP-Departement, CH-1211 Geneva 23, Switzerland

<sup>2</sup>Academia Sinica, Institute of Physics, Taipei, Taiwan

<sup>3</sup>CERN TH-Departement, CH-1211 Geneva 23, Switzerland

<sup>4</sup>SLAC National Accelerator Laboratory 2575 Sand Hill Rd., Menlo Park, CA, 94025  
USA

September 13, 2018

## Contents

<b>1</b>	<b>Context of the study</b>	<b>1</b>
<b>2</b>	<b>Bounds from HL-LHC</b>	<b>2</b>
<b>3</b>	<b>Discrimination from direct calculations</b>	<b>3</b>
<b>4</b>	<b>Discrimination from detector level analysis</b>	<b>4</b>
4.1	Leptonic analysis . . . . .	4
4.2	Hadronic analysis . . . . .	4
4.2.1	Results . . . . .	4
<b>5</b>	<b>Summary</b>	<b>5</b>

## Abstract

The 14 TeV LHC with  $L=3 \text{ ab}^{-1}$  of integrated luminosity can search for new  $Z'$  gauge bosons from the classic extended gauge theories up to masses of roughly  $\simeq 6 \text{ TeV}$ . Here we analyzed the capability of the 27 TeV HE-LHC with  $L=15 \text{ ab}^{-1}$  to distinguish among six  $Z'$  models employing only the  $e^+e^-$  and  $\mu^+\mu^-$  channels assuming that  $M_{Z'} = 6 \text{ TeV}$ . Under the assumption that these  $Z'$ 's decay only to SM particles, we show that there are sufficient observables to perform this model differentiation in most cases.

## 1 Context of the study

It is legitimate to assume that a heavy resonance could be seen at the end of High Luminosity LHC (HL-LHC). If that is the case a new collider with higher energy in the center of mass is needed to study its property as not enough events will be available at 14 TeV. In this document we present the discrimination potential of a High Energy LHC (HE-LHC) with a center of mass energy of 27 TeV.

Model	95% CL	$3\sigma$	$5\sigma$
SSM	6.62	6.09	5.62
LRM	6.39	5.85	5.39
$\psi$	6.10	5.55	5.07
$\chi$	6.22	5.68	5.26
$\eta$	6.15	5.59	5.16
I	5.98	5.45	5.05

Table 1:  $\sqrt{s} = 14$  TeV results for  $M_{Z'}$  in TeV as discussed in the text.

## 2 Bounds from HL-LHC

As a starting point it is needed to understand what are, for  $\sqrt{s} = 14$  TeV, for the typical exclusion/discovery reaches for some standard reference  $Z'$  models assuming  $L=3$   $\text{ab}^{-1}$  employing only the  $e^+e^-$  and  $\mu^+\mu^-$  channels. To address this and the other questions below we will use the same set of  $Z'$  models as employed in [1] and mostly in [2], both of which we will refer to frequently. We employ the MMHT2014 NNLO set [3] throughout with an appropriate constant  $K$ -factor ( $=1.27$ ) for numerics. The upper panel in Fig. 1 shows the production cross section times leptonic BF for these models at 14 TeV in the NWA. It has been and will be assumed here that these  $Z'$  states only decay to SM particles.

Using the present ATLAS and CMS results at 13 TeV, [4] and [5], it is straightforward to estimate by extrapolation the eventual 14 TeV exclusion reach in the combined  $e + \mu$  sample; this is given in the first column of Table 1. For discovery, only the  $e$  channel is used due to poor  $\mu$ -pair mass resolution near  $M_{Z'} = 6$  TeV although the muons will add some additional support for any observed excess as large masses. Estimates of the  $3\sigma$  evidence and  $5\sigma$  discovery limits are also given in the Table. Based on these results, we will assume in our study below that we are dealing with a  $Z'$  of mass 6 TeV; somewhat smaller mass choices will lead to very similar conclusions based on the ratio of predicted event rates shown in the lower panel of Fig. 1. Fig.2 shows the NWA cross sections for the same set of models but now at 27 TeV; with  $L=15$   $\text{ab}^{-1}$ , we note that very large statistical samples will be available for the case of  $M_{Z'} = 6$  TeV for each dilepton channel.

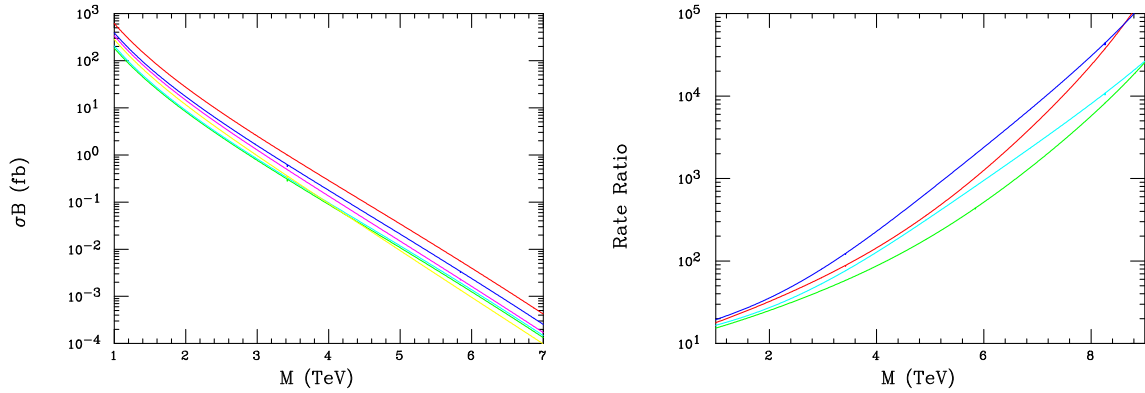


Figure 1: (Top)  $\sigma B_l$  in the NWA for the  $Z'$  production at the  $\sqrt{s} = 14$  TeV LHC as functions of the  $Z'$  mass: SSM(red), LRM (blue),  $\psi$ (green),  $\chi$ (magenta),  $\eta$ (cyan), I(yellow). (Bottom) Ratio of the number of events for  $\sqrt{s} = 27$  TeV,  $L=15$   $\text{ab}^{-1}$  to that at 13[14] TeV,  $L=3$   $\text{ab}^{-1}$  for  $\bar{u}u$  (red) and  $\bar{d}d$  (blue) [green, cyan] initial state partons with fixed invariant mass  $M$ .

### 3 Discrimination from direct calculations

Question: Can we use just this dilepton channel to distinguish between these six  $Z'$  models?

We make use of 3 observables, all in NWA:  $\sigma B_l$ , the forward-backward asymmetry,  $A_{FB}$  and the rapidity ratio,  $r_y$ . These last two are defined and discussed at some extent in both [1] and [2]. Given the ATLAS and CMS analyses as presented in [6] and [7] we employ the entire range of rapidity  $|y| \leq 2.5$  in defining these quantities. Based on these same works and [2], In addition to usual statistical errors, we will assume a 2% systematic error on the two ratios as most uncertainties (lumi and PDF) will cancel between numerators and denominators. For  $\sigma B_l$ , we assign a 5% systematic error in addition to this 2%; all errors are then added in quadrature. I am aware that these may be aggressive numbers but the plots will tell all.

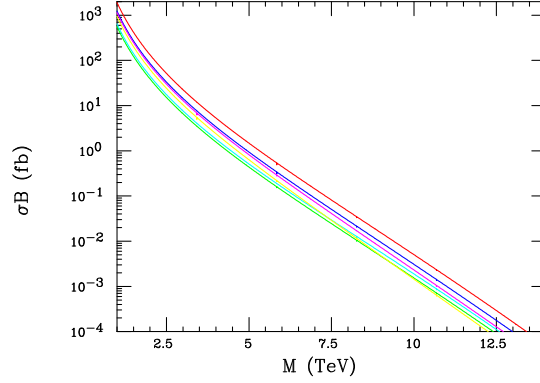


Figure 2: Same as the top panel in the previous Figure but now for the HE-LHC.

Fig. 3 shows the correlated predictions for these 3 observables for these six models given the above assumptions and employing *only* a single dilepton channel. Here we see that apart from a possible near degeneracy in models  $\psi, \eta$ , a reasonable  $Z'$  model separation is indeed achieved. It is clear that this remains possible even with somewhat larger values for the systematic errors. I note again that the use of  $\sigma B_l$  relies on the absence of new non-SM decay modes.

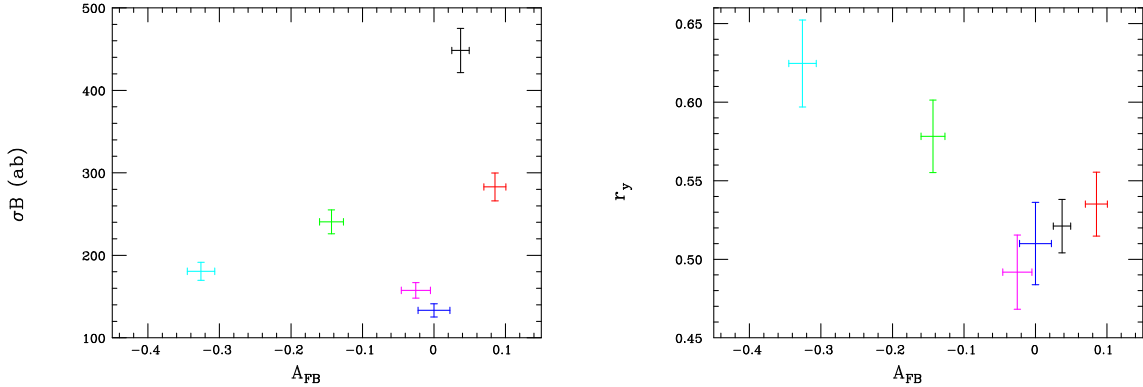


Figure 3: (Top)  $\sigma B_l$  vs  $A_{FB}$  and (Bottom)  $r_y$  vs  $A_{FB}$  at the HE-LHC assuming  $M'_Z = 6$  TeV as discussed in the text. SSM(black), LRM(red),  $\psi$  (blue),  $\chi$  (green),  $\eta$  (magenta) and I (cyan).  $1\sigma$  errors only are shown.

## 4 Discrimination from detector level analysis

The analyses presented in this section are all performed within the FCC software framework, FCCSW [8]. The detector parametrisation considered in this study is from HE-LHC official parametrisation for the yellow report [9].

### 4.1 Leptonic analysis

Events are required to contain at least two leptons with  $p_T > 0.5$  TeV,  $|\eta| < 4$ .

Figure 4 shows the invariant mass for a 6 TeV signal for the  $ee$  (left) and  $\mu\mu$  channels (right). The mass resolution is better for the  $ee$  channel, as expected from calorimetry. Several proxies for the true resonance mass have been tested, such as the invariant mass of the two taus, with and without correction for the missing energy. The transverse mass provided the best sensitivity and was therefore used to set limits and determine the discovery reach.

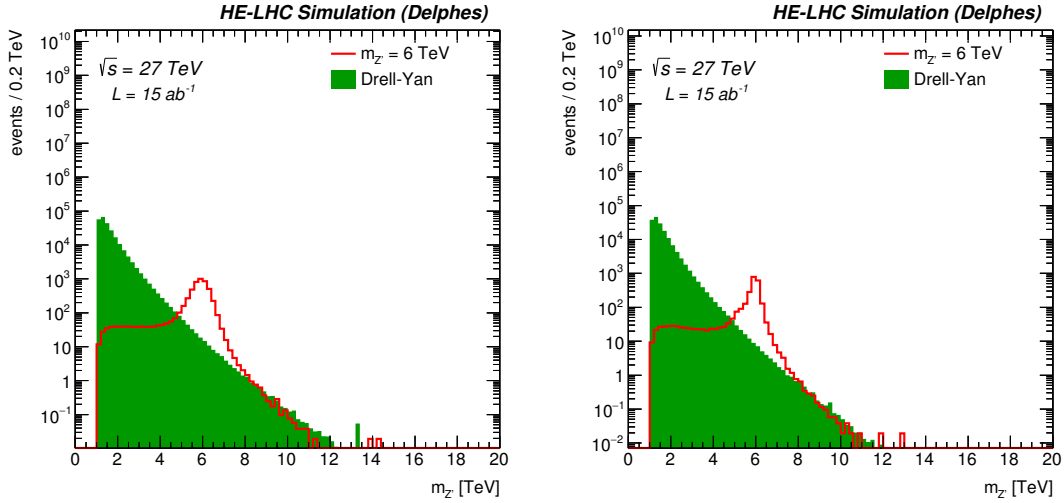


Figure 4: Invariant mass for a 6 TeV signal after full event selection for  $ee$  channel (left) and  $\mu\mu$  channel (right).

show  $y_Z$  plot explain AFB and  $r_y$

impact of  $\eta$  cut impact of ISR/SFR

### 4.2 Hadronic analysis

In this section the hadronic decays of the  $Z'$  will be tested in order to enhance the discrimination potential.

#### 4.2.1 Results

The model discrimination achieved by the hadronic analyses for 4, 6 and 8 TeV considering an integrated luminosity of 5, 15 and  $30\text{ab}^{-1}$  respectively is shown on Fig. ??, ??, 6. From the leptonic analysis 4.1, it was shown that for  $r_y$  For all cases, except for a mass of 8 TeV and an integrated luminosity of  $5\text{ab}^{-1}$ , discrimination is obtained at more than one sigma for the di-jet case.

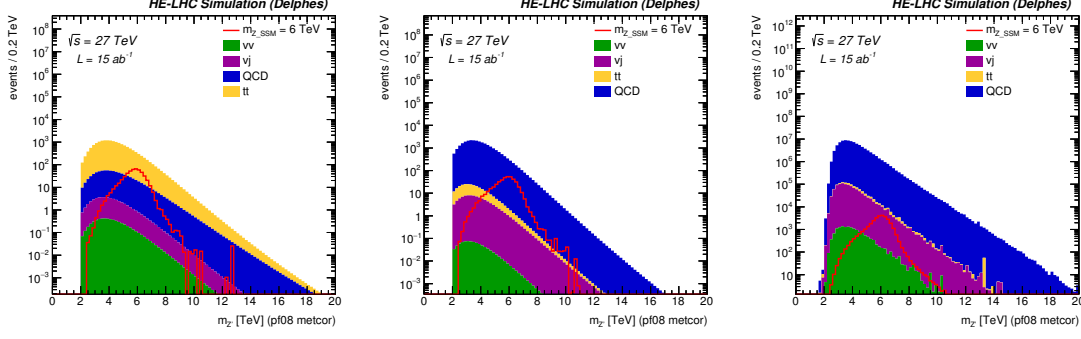


Figure 5: Left, center: Invariant mass for a 6 TeV signal after full event selection for  $ee$  channel (left) and  $\mu\mu$  channel (center). Right: Transverse mass for a 6 TeV signal after full event selection for the  $\tau\tau$  channel.

## 5 Summary

## Acknowledgements

This work was supported by the Department of Energy, Contract DE-AC02-76SF00515.

## References

- [1] T. G. Rizzo, Phys. Rev. D **89**, no. 9, 095022 (2014) doi:10.1103/PhysRevD.89.095022 [arXiv:1403.5465 [hep-ph]].
- [2] T. Han, P. Langacker, Z. Liu and L. T. Wang, arXiv:1308.2738 [hep-ph].
- [3] L. A. Harland-Lang, A. D. Martin, P. Motylinski and R. S. Thorne, Eur. Phys. J. C **75**, no. 5, 204 (2015) doi:10.1140/epjc/s10052-015-3397-6 [arXiv:1412.3989 [hep-ph]].
- [4] M. Aaboud *et al.* [ATLAS Collaboration], JHEP **1710**, 182 (2017) doi:10.1007/JHEP10(2017)182 [arXiv:1707.02424 [hep-ex]].
- [5] A. M. Sirunyan *et al.* [CMS Collaboration], arXiv:1803.06292 [hep-ex].
- [6] J. Han [ATLAS and CMS Collaborations], PoS ICHEP **2016**, 677 (2016).
- [7] CMS Collaboration [CMS Collaboration], CMS-PAS-SMP-16-007.
- [8] FCCSW main page, <http://fccsw.web.cern.ch/fccsw/>
- [9] HE-LHC twiki <https://twiki.cern.ch/twiki/bin/view/LHCPhysics/HLHELHCWorkshop>

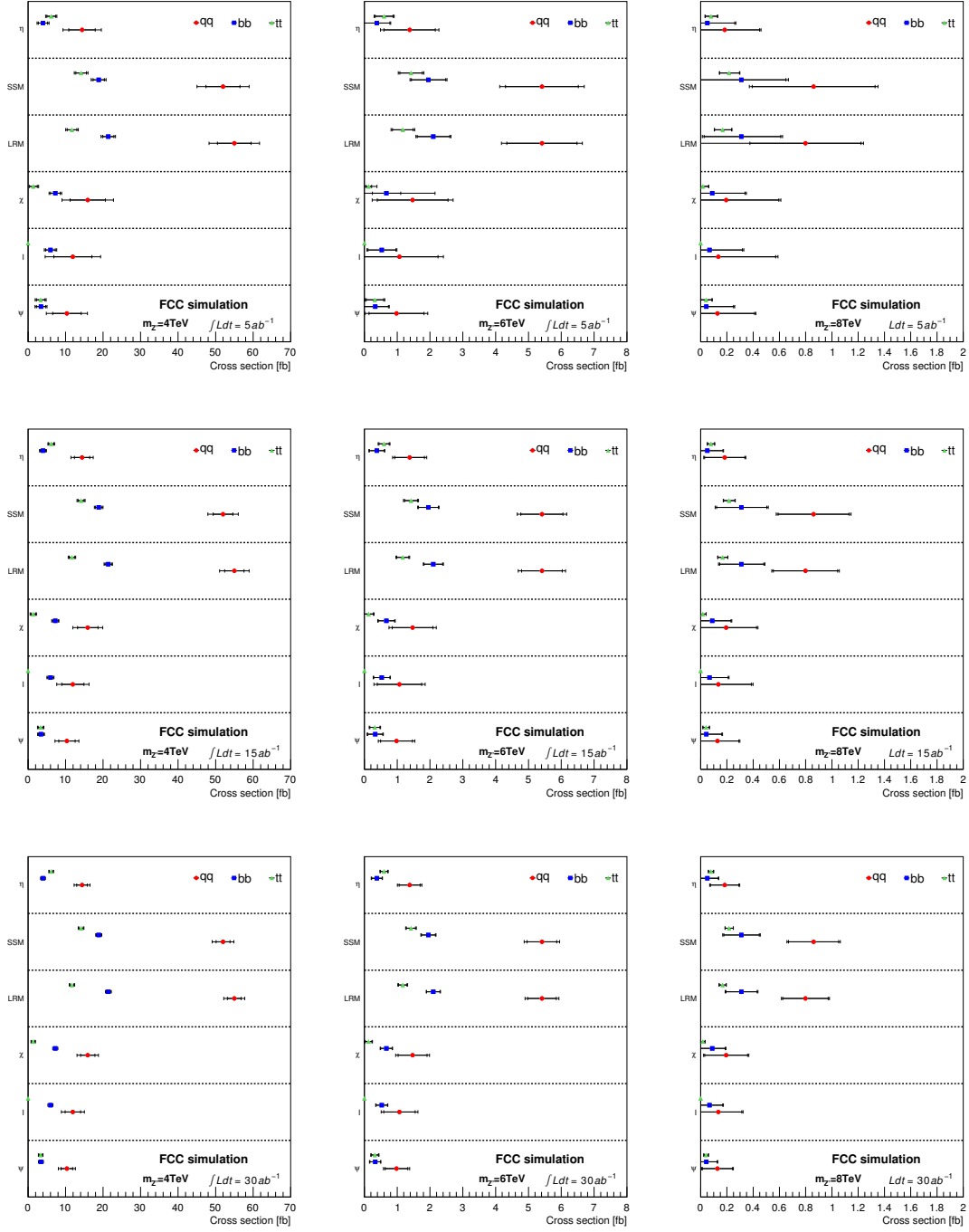


Figure 6: Discrimination for 4, 6 and 8 TeV (left, center, right) masses with 5, 15 and 30  $ab^{-1}$  (up, middle, down) of integrated luminosity. Statistical and full uncertainties are shown on each point.